

A Nonlinear Oscillator Network Circuit for Image Segmentation with Double-threshold Phase Detection

Hiroshi Ando, Makoto Miyake, Takashi Morie,
Makoto Nagata, and Atsushi Iwata

Faculty of Engineering, Hiroshima University, JAPAN

Summary:

This paper proposes a new image segmentation processing method using oscillator networks. Accurate image segmentation in the time domain is achieved by introducing a new double-threshold phase detection processing. We also propose LSI circuits for the oscillator network and the new segmentation processing using pulse modulation circuit techniques. Because some of the circuit components of the original oscillator network can be used for the new processing circuit, very few additional parts are necessary, and the circuit area is almost the same as in the original model.

1 Introduction

The segmentation of a visual image into a set of coherent patterns is a fundamental task in image processing. With the recent technological advances in single-object recognition, this task has become increasingly important. Moreover, real image segmentation has become important in the fields of image processing and data communication because the next generation video/audio coding format, MPEG-4, proposes object-base coding in which the figure and the background are processed separately.

D. L. Wang and D. Terman have proposed the *locally excitatory, globally inhibitory oscillator networks (LEGION)* as a practical model for image segmentation using a nonlinear oscillator system [1, 2]. Image segmentation using oscillator networks has some advantages when compared with other models, e.g., automatic labeling of patterns in the time domain.

However, in the original LEGION model, the relation between the oscillator state and the segmentation result is not clear because

the former is in analog while the latter utilizes binary values. An aim of the present paper, therefore, is to propose a superior segmentation processing method using oscillator networks.

As a related issue, in order to apply the LEGION model to real-time image or moving picture segmentation, VLSI implementation is essential because the LEGION model requires highly parallel, complicated, nonlinear operations. We have already proposed circuit architectures for arbitrary nonlinear dynamical systems using pulse modulation techniques [3, 4]. Based on these architectures, we have also proposed circuits for a nonlinear oscillator portion of the LEGION model [5, 6]. Accordingly, a second aim of this paper is to propose LSI circuits for the whole oscillator network and for the new segmentation processing.

2 Image segmentation using oscillator networks

2.1 Oscillator network model

Schematics of the LEGION model are shown in Fig. 1. This model is slightly modified from the original one [2] in order to allow for gray-level image segmentation. The model consists of a large number of oscillators, each corresponding to a respective image pixel, and a global inhibitor. Each oscillator is connected to the neighboring oscillators and the global inhibitor, which is a suitable structure for VLSI implementation from the viewpoint of interconnection complexity.

The dynamics of the i -th oscillator are represented by the following equations:

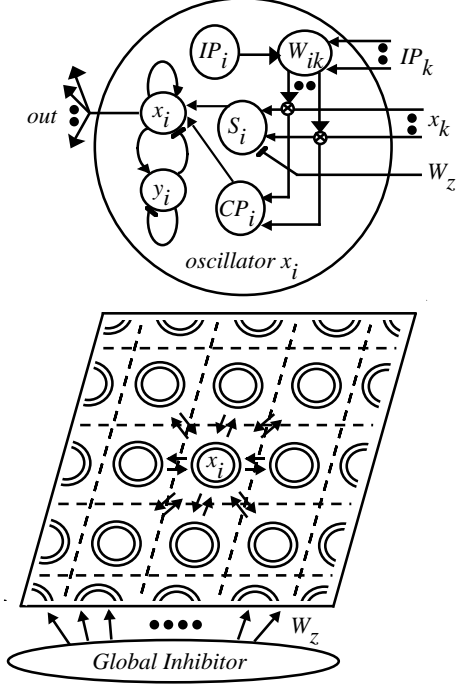


Figure 1: Oscillator network model.

$$\frac{dx_i}{dt} = 3x_i - x_i^3 + 2 + \rho - y_i + \alpha H(CP_i) + H_2(S_i), \quad (1)$$

$$\frac{dy_i}{dt} = \varepsilon[\gamma(1 + \tanh(x_i/\beta)) - y_i], \quad (2)$$

where ρ , α , ε , γ and β are constants; CP_i is a variable determined by the image data; S_i is

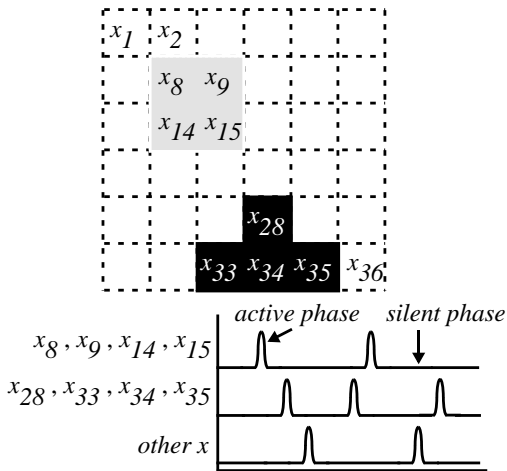


Figure 2: Oscillator network state.

a coupling term described below; and $H(x)$ and $H_2(x)$ are defined as $H(x) = 1$, $H_2(x) = 1$ if $x \geq 0$ and $H(x) = 0$, and $H_2(x) = -1$ if $x < 0$. The oscillator state is expressed by the variable x_i . These dynamics produce active and silent phases in each oscillator, and synchronous and asynchronous states between oscillators, as shown in Fig. 2. A region oscillating synchronously is extracted as a coherent pattern. Whether or not an oscillator belongs to an oscillation region is determined by whether $H_2(S_i)$ is positive or negative in Eq. (1). The S_i and CP_i terms are given by

$$S_i = \sum_{k \in N_i} W_{ik} H(x_k - \theta_x) - W_z H(z - \theta_z), \quad (3)$$

$$CP_i = \sum_{k \in N_i} W_{ik} - \theta_p, \quad (4)$$

where W_z , θ_x , θ_z and θ_p are constants, and N_i is the neighborhood of i . The connection weight W_{ik} from oscillator k to i is given by

$$W_{ik} = \frac{imax}{1 + |IP_i - IP_k|}, \quad (5)$$

where IP_i is the image intensity at pixel i , and $imax$ is the maximum intensity value (255 for 8bit data). The global inhibitor state z in Eq. (3) is given by

$$z = H\left(\sum_i H(x_i - \theta_{xz}) - 1\right), \quad (6)$$

where θ_{xz} is a constant.

The dynamics for segmentation are as follows. When pixel i and k belong to a coherent pattern, weight W_{ik} becomes large because $|IP_i - IP_k|$ is small. Oscillators i and k oscillate synchronously because $H_2(S_i)$ in Eq. (1) becomes unity. On the other hand, oscillators i and k oscillate asynchronously when they belong to neighboring different coherent patterns because W_{ik} becomes small. In this way, regions corresponding to different neighboring coherent patterns are separated from each other.

2.2 Double-thresholding method for improving image segmentation

The states of oscillators are represented by analog values, but the information for image segmentation should consist of binary

DEVICE

(a) input image

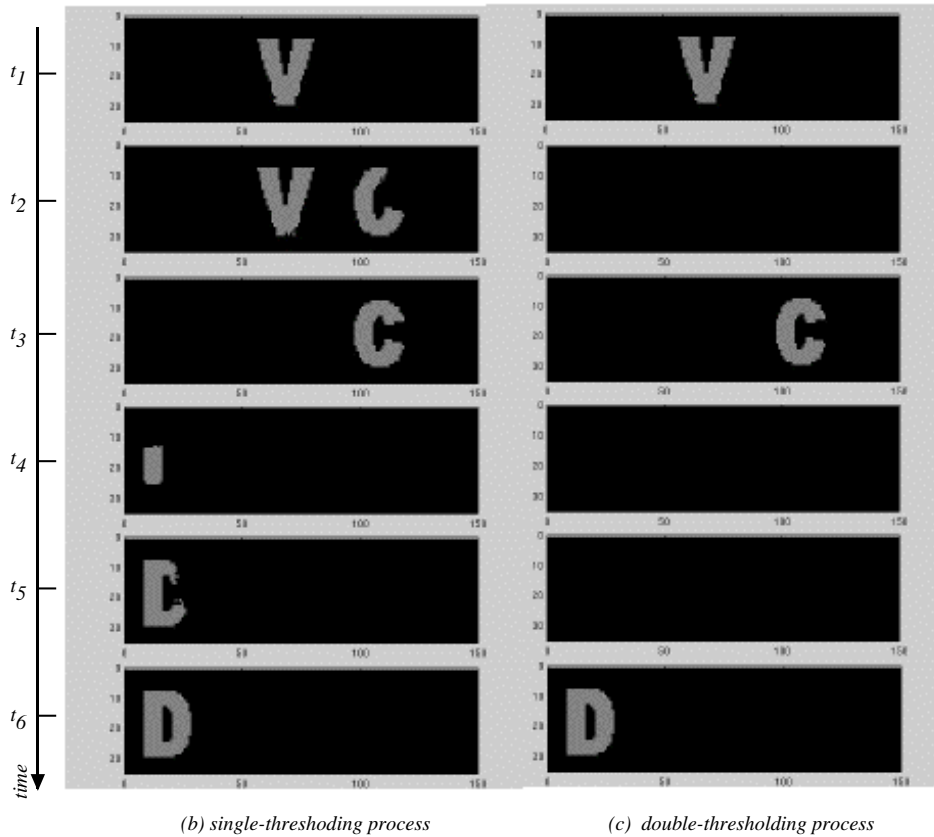


Figure 3: Input image and snapshots of oscillator activities $\{\phi(x_i)\}$.

values. We define a binary variable $\phi(x_i)$ as an activity of oscillator i , which determines whether pixel i is included in the active image region.

Thresholding is a simple method for obtaining binary data from analog data: $\phi(x_i) = H(x_i - \theta_1)$, where $H(\cdot)$ is the same step function defined in the previous section, and θ_1 is the threshold. In the previous reports [5, 6], image segmentation by oscillator networks was performed using this process. An example of the simulation results is shown in Fig. 3(b). As time passes, the coherent regions gradually appear; for example, letter ‘‘C’’ appears at from t_2 to t_3 , and letter ‘‘D’’ appears at from t_4 to t_6 . Moreover, plural coherent regions happen to appear at t_2 . The relationship between oscillator states $\{x_i\}$ and activities $\{\phi(x_i)\}$ in

such situations is shown in Fig. 4(a). Here, the variables x_i , x_j and x_k correspond to the three oscillators indicated within the white circles of letters ‘‘C’’ and ‘‘V’’, respectively. As shown Fig. 3(b), it is difficult to determine the timings when only one coherent region is perfectly extracted from the continuously changing output.

In order to solve this problem, we propose a double-threshold processing. We introduce the second threshold parameter θ_2 , and define the activity inhibition region using both thresholds. When at least one oscillator stays at the inhibition region, that is, $\theta_2 < x_i < \theta_1$, all $\phi(i)$ ’s are set at 0, as shown in Fig. 4(b). As a result, $\phi(i) = \phi(j) = \phi(k) = 0$ at t_2 , while $\phi(k)$, $\phi(i)$ and $\phi(j)$ still appear at t_1 and t_3 . The numerical simulation results shown in Fig. 3(c)

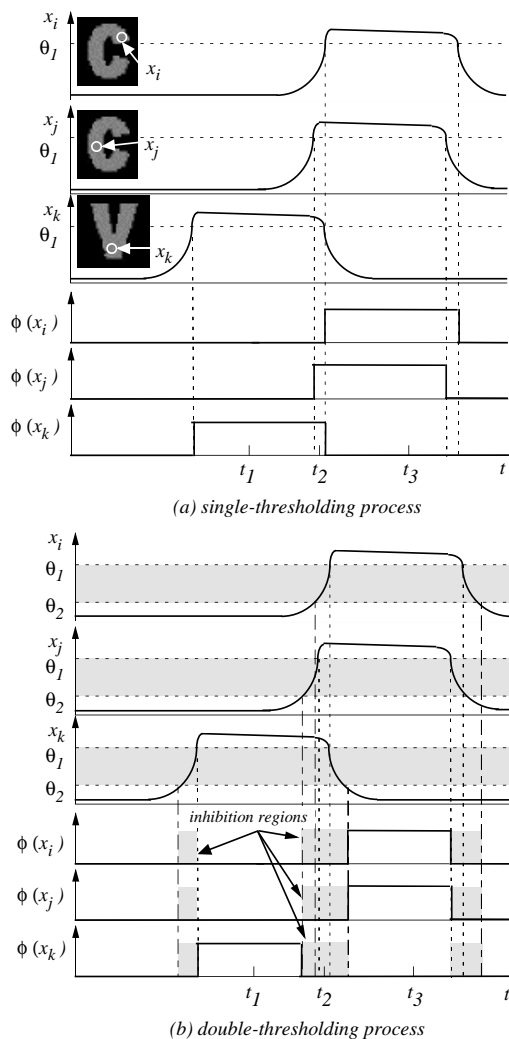


Figure 4: Relationship between oscillator states $\{x_i\}$ and activities $\{\phi(x_i)\}$.

demonstrate perfect segmentation in this example. It is noted that even when using the new method, plural coherent regions are extracted together if no oscillators stay at the inhibition region and if $x_i > \theta_1$ for all oscillators belonging to the plural regions at the same time. However, the probability of this situation occurring is very low.

3 Circuits for image segmentation

3.1 Pulse modulation circuits for nonlinear dynamical system

The pulse modulation approaches achieve time-domain analog information processing using pulse signals. These approaches include pulse-width modulation (PWM) and pulse-phase modulation (PPM) methods. The PWM approach is suitable for large-scale integration of analog processing circuits because it matches the scaling trend in Si CMOS technology and leads to low voltage operation. This approach also achieves lower power consumption operation than traditional digital circuits because one data is represented by only one state transition. The PPM approach also has these advantages. However, the PPM approach requires a reference clock signal defining the start time for measuring the phase, whereas a PWM signal includes all this information independently. PWM signals are therefore suitable for signal transmission, whereas PPM methods can be used effectively in local circuits. Thus, pulse modulation approaches have been used in an analog-digital merged circuit architecture [7].

Figure 5 shows a circuit that can implement arbitrary nonlinear transformation. The input voltage is linearly transformed into a PWM signal V_a having a pulse width of T by comparing it with a linearly ramped signal V_{ramp} . Then, the PWM signal is transformed into the PPM signal V_b . The PPM signal switches a current source modulated by nonlinear non-monotone waveform $f(t)$. The current source supplies charges equal to $f(T)\Delta t$ to a serially connected capacitor C . As a result, the voltage of the capacitor node is nonlinearly modulated; the voltage change is $f(T)\Delta t/C$. If the output voltage is fed back to the input, this circuit can implement discrete-time dynamics. This is an approximate solution of the corresponding differential equation if the voltage change is very small. Thus, we can easily obtain nonlinearly modulated voltage and PWM/PPM signal trains following arbitrary nonlinear dynamics.

3.2 Oscillator network circuit

Oscillator circuit A nonlinear oscillator circuit using the PWM/PPM method is shown in Fig. 6. This circuit implements the dynamics expressed by Eqs. (1) and (2). The values of x_i and y_i are represented by voltages V_{x_i} and V_{y_i} , and are stored as charges in capacitors C_{x_i} and C_{y_i} , respec-

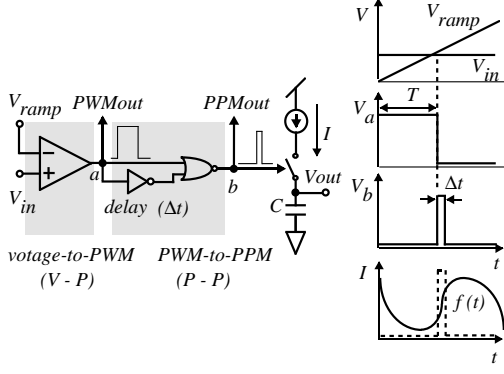


Figure 5: Nonlinear transformation circuit using pulse modulation.

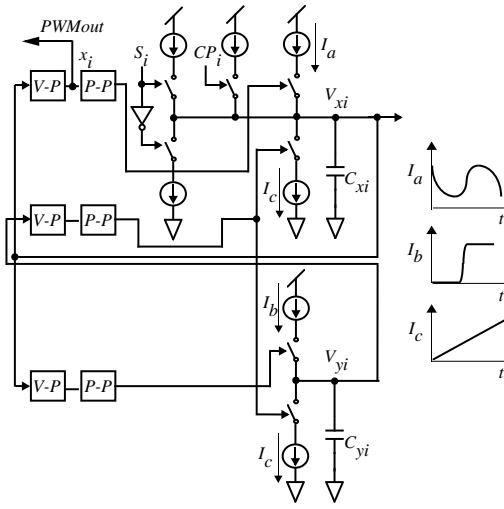
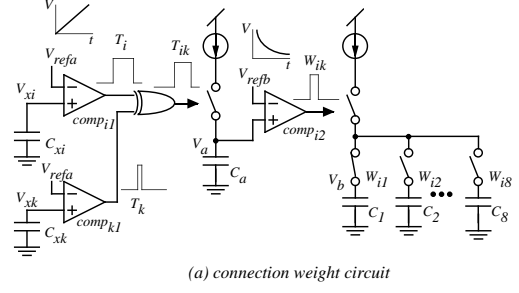


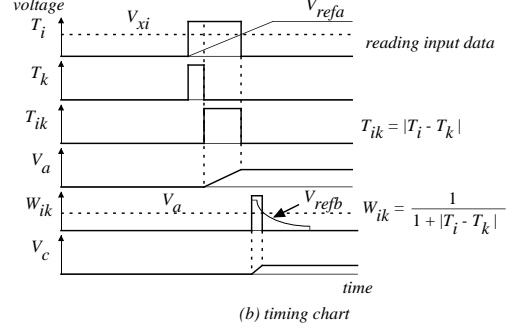
Figure 6: Oscillator circuit.

tively. The third-order and tanh functions of x_i in Eqs. (1) and (2) are generated by conversion from voltage into PPM signals and the nonlinearly modulated current sources. The PPM signals switch current sources, and small charges corresponding to finite differences in Eqs. (1) and (2) are injected into or extracted from C_{xi} and C_{yi} in each time step.

A threshold function $H(\cdot)$ as used in Eqs. (1), (3) and (6) is easily generated by using a comparator. Since summations and multiplications are easily performed by using switched current sources as shown in Fig. 6, calculations given by Eqs. (1) to (6) except (5) (see below) are easily performed.



(a) connection weight circuit



(b) timing chart

Figure 7: Connection weight circuit.

Connection Weight Circuit The connection weights expressed by Eq. (5) are obtained by the circuit shown in Fig. 7. Image intensity IP_i is assumed to be given by voltage V_{xi} . The voltage V_{xi} is linearly transformed into a pulse with a width of T_i by comparator $comp_{i1}$. The absolute difference between IP_i and the neighboring pixel data IP_k , $|IP_i - IP_k|$ is generated by an XOR logic gate as a PWM pulse T_{ik} . The pulse is transformed into voltage V_a , and V_a is compared with a reference signal voltage V_{refb} that varies in the time domain: $V_{refb}(t) = 1/t - 1$. The pulse width of the comparator output, W_{ik} , is obtained by $V_{refb}(W_{ik}) = 1/W_{ik} - 1 = V_a$. Since V_a is proportional to $|IP_i - IP_k|$, W_{ik} expressed by Eq. (5) is obtained, and the results for eight neighborhoods are stored in capacitors C_{ik} , ($k = 1, \dots, 8$), respectively.

3.3 Double-thresholding circuit for image segmentation

The double-thresholding circuit described in Sec 2.2 is shown in Fig. 8. The operations $H(x_i - \theta_1)$ and $H(x_i - \theta_2)$ are performed by $comp_{i1}$ and $comp_{i2}$, respectively. The XOR gate output V_i is “High” only when $\theta_2 < V_{xi} < \theta_1$. This process is performed for

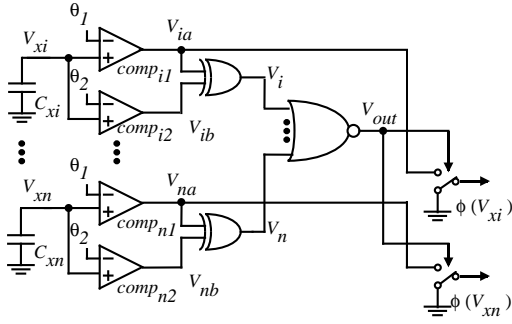


Figure 8: Double-thresholding circuit.

all oscillators simultaneously. Therefore, the NOR output V_{out} is “Low” if the following inequalities are valid for at least one oscillator: $\theta_2 < V_{xi} < \theta_1$. When V_{out} is “Low”, all activities $\{\phi(V_{xi})\}$ are set at zero. Thus, we can perform the double-thresholding process.

We can commonly use comparators for the connection weight circuit and for the double-thresholding circuit. We can also use connections with all oscillators for the global inhibitor and for this circuit. For this reason, very few additional circuit components are required for this new double-threshold processing, and the pixel size is almost the same as for the original model.

4 Conclusion

We proposed a new image segmentation method using nonlinear oscillator networks. By introducing a new double-threshold processing and inhibition periods into the activities of oscillators, accurate image segmentation in the time domain is achieved. Using the new segmentation process, only one coherent region is extracted at a time, and no region is extracted during the transient period for extraction.

We also proposed circuit blocks for the oscillator network and the new segmentation processing using pulse modulation circuit techniques. The LSI circuit design for the image segmentation system is in progress.

Acknowledgments

This work was supported by Grant-in-aid #11555102 for Scientific Research from the

Ministry of Education, Science and Culture of Japan. This work was also supported in part by Grants-in-aid for the Core Research for Evolutional Science and Technology (CREST) from the Japan Science and Technology Corporation (JST).

References

- [1] D. L. Wang and D. Terman, “Locally Excitatory Globally Inhibitory Oscillator Networks,” *IEEE Trans. Neural Networks*, vol. 6, no. 1, pp. 283–286, 1995.
- [2] D. L. Wang and David Terman, “Image Segmentation Based on Oscillatory Correlation,” *Neural Computation*, vol. 9, no. 4, pp. 805–836, 1997.
- [3] T. Morie, S. Sakabayashi, M. Nagata, and A. Iwata, “Nonlinear Function Generators and Chaotic Signal Generators Using a Pulse-Width Modulation Method,” *Electron. Lett.*, vol. 33, no. 16, pp. 1351–1352, 1997.
- [4] T. Morie, S. Sakabayashi, H. Ando, M. Nagata, and A. Iwata, “Pulse Modulation Circuit Techniques for Nonlinear Dynamical Systems,” in *Proc. Int. Symp. on Nonlinear Theory and its Application (NOLTA’98)*, pp. 447–450, Crans-Montana, Sept. 1998.
- [5] T. Morie, H. Ando, S. Sakabayashi, M. Nagata, and A. Iwata, “A New PWM Technique Implementing Arbitrary Nonlinear Dynamics and its Application to Oscillator Neurons,” in *The 2nd R. I. E. C. Int. Symposium on Design and Architecture of Information Processing Systems Based on The Brain Information Principles (DAIPS)*, pp. 275–278, Sendai, March 1998.
- [6] H. Ando, T. Morie, M. Nagata, and A. Iwata, “Oscillator Networks for Image Segmentation and their Circuits using Pulse Modulation Methods,” in *Proc. 5th Int. Conf. on Neural Information Processing (ICONIP’98)*, pp. 586–589, Kitakyushu, Oct. 1998.
- [7] A. Iwata and M. Nagata, “A Concept of Analog-Digital Merged Circuit Architecture for Future VLSI’s,” *IEICE Trans. Fundamentals.*, vol. E79-A, no. 2, pp. 145–157, 1996.